Neuron
Article

Single-Cell Optogenetic Excitation Drives Homeostatic Synaptic Depression

Carleton P. Goold[1,2] and Roger A. Nicoll[1,*]
[1]Departments of Cellular and Molecular Pharmacology and Physiology
[2]Neuroscience Graduate Program
University of California San Francisco, San Francisco, CA 94158, USA
*Correspondence: nicoll@cmp.ucsf.edu
DOI 10.1016/j.neuron.2010.09.020

SUMMARY

Homeostatic processes have been proposed to explain the discrepancy between the dynamics of synaptic plasticity and the stability of brain function. Forms of synaptic plasticity such as long-term potentiation alter synaptic activity in a synapse- and cell-specific fashion. Although network-wide excitation triggers compensatory homeostatic changes, it is unknown whether neurons initiate homeostatic synaptic changes in response to cell-autonomous increases in excitation. Here we employ optogenetic tools to cell-autonomously excite CA1 pyramidal neurons and find that a compensatory postsynaptic depression of both AMPAR and NMDAR function results. Elevated calcium influx through L-type calcium channels leads to activation of a pathway involving CaM kinase kinase and CaM kinase 4 that induces synaptic depression of AMPAR and NMDAR responses. The synaptic depression of AMPARs but not of NMDARs requires protein synthesis and the GluA2 AMPAR subunit, indicating that downstream of CaM kinase activation divergent pathways regulate homeostatic AMPAR and NMDAR depression.

INTRODUCTION

The balance of incoming excitatory and inhibitory synaptic activity governs the firing output of a neuron by controlling moment-to-moment fluctuations in membrane potential. Although synaptic plasticity can alter this balance and change neural activity on short time scales, over long time periods mean firing rates in pyramidal cells remain highly stable (Buzsaki et al., 2002). One well-studied form of synaptic plasticity, long-term potentiation (LTP), presents a theoretical problem for neural stability. LTP is triggered by correlated pre- and postsynaptic spiking and increases the strength of excitatory glutamatergic synapses in a synapse-specific manner. Since correlated spiking triggers LTP, the increased firing expected to result from LTP could initiate a runaway positive feedback cycle of further LTP and increased firing (Turrigiano and Nelson, 2000). Synaptic homeostasis has been hypothesized to restrain runaway plasticity and stabilize neural activity (Burrone and Murthy, 2003; Davis, 2006; Turrigiano and Nelson, 2000). In synaptic homeostasis, global alterations of synaptic strength are thought to compensate for deviations from optimal levels of neural activity (Burrone and Murthy, 2003; Turrigiano and Nelson, 2000).

Bidirectional homeostatic responses compensate for activity perturbations in both peripheral and central neurons. At the neuromuscular junction, inhibition of postsynaptic receptor function triggers a presynaptic increase in neurotransmitter release that restores muscle depolarization (Davis, 2006; Frank et al., 2006). In cortical and hippocampal neurons, network-wide blockade of spiking or glutamate receptor function induces compensatory enhancement of pre- or postsynaptic function (O'Brien et al., 1998; Thiagarajan et al., 2005; Murthy et al., 2001; Turrigiano et al., 1998). Similarly, elevating network activity with GABA receptor antagonists causes compensatory reductions of synaptic function (O'Brien et al., 1998; Turrigiano et al., 1998). Homeostatic systems are thought to require molecules to sense perturbations of activity, to execute compensatory changes and to couple these functions (Davis, 2006; Turrigiano, 2008). Several molecules, including dysbindin, ephexin, CaM kinases, and Arc have been implicated in these roles in the homeostatic response to activity blockade (Dickman and Davis, 2009; Frank et al., 2009; Ibata et al., 2008; Shepherd et al., 2006; Thiagarajan et al., 2002). Homeostatic responses to elevated activity require Polo-like kinase 2, which couples sensor activation and execution of compensatory changes (Seeburg et al., 2008). However, less is known about the mechanism by which a homeostatic program might sense elevated activity or execute compensatory responses to elevated activity. CaM kinases are attractive candidates for the homeostatic sensor of elevated activity, since pharmacological or genetic inhibition of CaM kinases occludes homeostatic responses to activity blockade (Haghighi et al., 2003; Ibata et al., 2008; Thiagarajan et al., 2002). Altered AMPA receptor (AMPAR) expression is thought to underlie the execution of homeostatic plasticity (Ibata et al., 2008; O'Brien et al., 1998; Turrigiano et al., 1998). Knockdown of the GluA2 AMPAR subunit (formerly known as GluR2) prevents synaptic scaling up after activity blockade (Gainey et al., 2009). It is unknown what role specific AMPAR subunits might play in homeostatic responses to elevated activity. Bidirectional, compensatory alterations of NMDAR surface expression and synaptic localization in response to activity perturbations have been documented using immunochemical and imaging techniques (Mu et al., 2003; Rao and Craig, 1997). However, very few studies have demonstrated functional alterations of synaptic

NMDARs in homeostatic plasticity (Watt et al., 2000), and it is unclear if common or distinct signaling pathways regulate AMPARs and NMDARs.

Inhibition of activity in individual pyramidal neurons using either local TTX perfusion (Ibata et al., 2008) or expression of the potassium channel Kir2.1 (Burrone et al., 2002) induces compensatory increases in synaptic function. Enhancing activity in individual neurons can alter axon initial segment position, a marker of intrinsic excitability (Grubb and Burrone, 2010). However, homeostatic changes in synaptic function in response to elevated activity have only been studied using network-wide manipulations. It is thus unknown if the sensors that detect elevated activity and initiate compensatory alterations of synaptic function are contained within individual neurons, or whether collective network activation or nonneural signals such as TNFα (Stellwagen and Malenka, 2006) are necessary for homeostatic responses to elevated activity. This question is especially important in order to address whether synaptic homeostasis can respond to synapse-specific forms of synaptic potentiation such as LTP. Additionally, a mechanistic understanding of homeostatic responses to elevated activity will help identify how these processes might go awry in diseases of excess neural activity such as epilepsy.

To test whether neurons homeostatically respond to cell-autonomous increases in activity, we employed an optogenetic excitation system using photostimulation of Channelrhodopsin 2 (ChR2)-expressing CA1 pyramidal neurons. We find that a compensatory synaptic depression of both AMPAR and NMDAR responses occurs after 24 hr of stimulation and involves a postsynaptic elimination of synapses. We show that calcium influx through L-type voltage gated calcium channels is required for the synaptic depression. Increased calcium influx, elicited either by ChR2-photostimulation or enhanced network synaptic activity, induces compensatory depression through a pathway involving CaMKK, CaMK4 and protein translation. CaMKK and CaMK4 activation regulate both AMPAR and NMDAR depression. However, downstream of CaMK4 activation, divergent signaling pathways control the depression of AMPARs and NMDARs. These results outline a molecular mechanism whereby neurons can cell-autonomously sense and respond to elevated activity. Further, cell-autonomous optogenetic manipulation represents a robust new method for the study of synaptic homeostasis.

RESULTS

Excitation System Design

To render neurons excitable by light, we expressed the algal light-gated cation channel ChR2 in organotypic rodent hippocampal slices using sparse biolistic transfection (Nagel et al., 2003; Boyden et al., 2005; Zhang and Oertner, 2007). By doing so, depolarization of ChR2-expressing neurons can be tuned with light illumination of varying intensity and timing (Boyden et al., 2005). We used organotypic slices because: (1) they facilitate long optical and pharmacological manipulations; (2) they allow simultaneous dual whole-cell recording to rigorously compare synaptic transmission between control and genetically manipulated neurons; and (3) they retain much of the native hippocampal architecture and are considered to maintain more native cellular properties than dissociated culture (Caeser and Aertsen, 1991).

To validate our photostimulation method as a tool to chronically excite neurons, we first characterized the direct effect of light stimulation on ChR2-transfected pyramidal cells. ChR2-transfected CA1 pyramidal cells were identified by mCherry fused to ChR2. As expected, light pulses evoked inward currents (Figure 1A) in ChR2-transfected neurons (blue trace) voltage-clamped at negative holding potentials, but not in simultaneously recorded control cells (black trace). In selecting a stimulation protocol, we explored frequencies (1–3 Hz) that roughly double to quadruple average firing frequency recorded in CA1 neurons (~1 Hz), but which are below peak firing rates (~10 Hz) (Ahmed and Mehta, 2009). We used 50 ms pulses to mimic the long depolarization that underlies complex spike bursts (Kandel and Spencer, 1961), which encompass a substantial proportion of total spikes recorded in vivo (Harris et al., 2001). To observe the effect of light pulses on ChR2-transfected membrane potential and on overall slice activity, we performed simultaneous current-clamp recordings from ChR2-transfected and control neurons. Transfected neurons faithfully followed trains of 3 Hz 50 ms light pulses with trains of large EPSP-like depolarizations (Figure 1B). By contrast, minimal activity was synchronously evoked in control cells, even though transfected neurons presumably release neurotransmitter in response to depolarization-triggered action potentials. This is most likely due to the extremely low efficiency of biolistic transfection (typically 1–10 pyramidal cells/slice) and consequent low probability of any given control cell receiving synapses from a ChR2-transfected cell.

Cell-Autonomous Effects of Chronic Excitation on Excitatory but Not Inhibitory Synapses

To examine whether ChR2 expression, in the absence of light, altered the amplitude of synaptic currents, we compared synaptic responses to a shared presynaptic Schaffer collateral input on adjacent ChR2-transfected and control neurons (see diagram in Figure 1C). There was no change in AMPAR responses recorded at −70 mV (AMPAR $I_{transfected}/I_{control}$ = 1.07 ± 0.18; n = 12 pairs; $p > 0.75$; Figure S1A available online). Similarly, NMDAR-mediated currents in compound EPSCs at +40 mV, measured 100 ms poststimulus, were also unaffected (NMDAR $I_{transfected}/I_{control}$ = 1.03 ± 0.36; n = 12; $p > 0.9$).

To examine the effect of chronic excitation on synaptic responses, we stimulated ChR2-transfected slices with 50 ms blue light pulses at 3 Hz for 12 or 24 hr, then measured synaptic responses. After 12 hr of light stimulation, neither AMPAR nor NMDAR currents significantly decreased in ChR2-transfected relative to adjacent control neurons (Figure S1A). After 24 hr of light stimulation, however, both AMPAR ($I_{transfected}/I_{control}$ = 0.48 ± 0.05; n = 37; $p < 10^{-5}$; Figure 1D1) and NMDAR responses in compound EPSCs ($I_{transfected}/I_{control}$ = 0.40 ± 0.07; n = 27; $p < 0.0005$; Figure 1D2) were profoundly depressed in ChR2-transfected, photostimulated neurons. (Hereafter, we refer to ChR2-transfected neurons in slices photostimulated for 24 hr as "photostimulated neurons") We also measured isolated NMDAR responses in photostimulated neurons in the presence

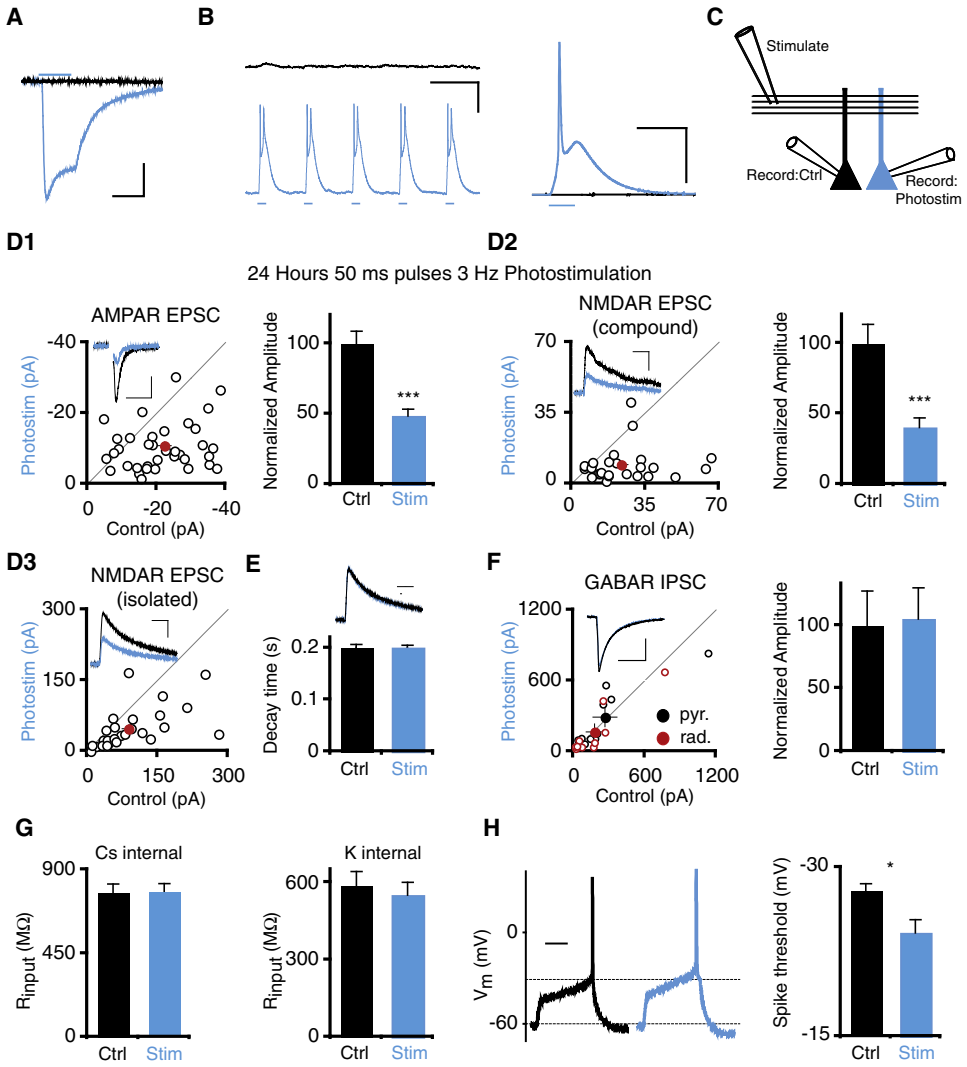

Figure 1. Twenty-Four Hour Photostimulation Induces Depression of AMPAR and NMDAR Synaptic Responses in CA1 Pyramidal Cells

(A) Voltage-clamp recording at −70 mV of inward current induced by 50 ms blue light pulse on ChR2-transfected CA1 pyramidal cell (blue trace) and simultaneously recorded control cell (black trace). Scale bar represents 50 ms, 100 pA.

(B) (Left) Single sweep from simultaneous current-clamp recording of ChR2-transfected and control cell. Blue light pulses elicit sustained trains of depolarizations in ChR2 cells. Scale: 333 ms, 25 mV. (Right) Average of 80 traces during 50 ms light pulses from different ChR2- and control cell pair, recorded simultaneously. Light does not evoke synaptic activity in the control cell. Scale bar represents 100 ms, 25 mV.

(C) Recording configuration. Synaptic responses to a shared presynaptic input in ChR2-transfected and control neurons are compared using simultaneous whole-cell recording.

(D) Scatter plot of EPSCs from single pairs (open circles) and mean ± standard error of mean (SEM) (red circle) of simultaneously recorded ChR2-transfected (Stim) and control neurons (Ctrl) from slices photostimulated 24 hr with 50 ms light pulses at 3 Hz. Photostimulation causes a significant depression of both AMPAR and NMDAR responses in ChR2-transfected neurons. Insets are representative traces. (D1) AMPAR EPSCs recorded at −70 mV. (D2) Compound EPSCs recorded at +40 mV. NMDAR response is measured 100 ms after stimulus. (D3) Pharmacologically isolated NMDAR response recorded at +40 mV, measured at peak. Scale bars represent: D1: 50 ms, 10 pA; D2: 100 ms, 20 pA; D3: 100 ms, 50 pA. *$p < 0.05$, **$p < 0.01$; ***$p < 0.001$.

(E) No change in decay time constants of NMDAR responses. Inset: representative scaled NMDAR responses. Scale bar represents 100 ms.

(F) Scatter plot of IPSCs. IPSCs were elicited with stimulating electrodes positioned either in stratum pyramidale or radiatum. Open circles represent single pairs, closed circles mean ± SEM. Graph shows normalized mean amplitude ± SEM for pooled IPSCs; there is no significant change in IPSC amplitude in ChR2-transfected neurons versus control neurons. Scale bar represents 100 ms, 300 pA.

(G) Input resistance, measured using Cs- or K-based internal solution. There is no significant difference between photostimulated and control neuron input resistance in either condition.

(H) Photostimulated neurons have a significantly more depolarized threshold for action potential threshold. (Left) Representative traces, showing response to minimal current injection necessary to elicit action potentials in control and photostimulated neuron. Scale bar represents 200 ms. See also Figure S1.

of NBQX and found similar results ($I_{transfected}/I_{control}$ = 0.55 ± 0.08; n = 35; p < 0.0002; Figure 1D3). Since synaptic activity can alter NMDAR subunit composition and decay kinetics (Bellone and Nicoll, 2007) we measured the decay time constant of isolated NMDAR responses to determine if any similar alteration of subunit composition occurred in response to photostimulation. However, we found no difference in NMDAR decay time constants between photostimulated and control cells (control: 0.20 ± 0.01 s; transfected: 0.20 ± 0.01 s; Figure 1E). Stimulation at 1 Hz for 24 hr also induced synaptic depression of both AMPAR and NMDAR responses (Figure S1A). We used 3 Hz stimulation for all subsequent experiments since it produced more robust effects.

Chronic enhancement of hippocampal network activity triggers alterations in inhibitory GABAR synaptic transmission (Otis et al., 1994; Wierenga and Wadman, 1999). In parallel with compensatory changes in excitatory transmission, these compensatory alterations in inhibition have been hypothesized to help restrain neural activity (Turrigiano and Nelson, 2000). To determine if cell-autonomous enhancement of activity can modify inhibitory strength, we measured GABAR IPSCs in photostimulated neurons by recording currents evoked by direct stimulation of inhibitory cells either in stratum radiatum or pyramidale in the presence of the AMPAR and NMDAR antagonists NBQX and D-APV. We did not observe changes in inhibitory currents originating from either layer (radiatum $I_{transfected}/I_{control}$ = 0.93 ± 0.39; n = 10; p > 0.6; pyramidale $I_{transfected}/I_{control}$ = 1.09 ± 0.31; n = 10; p > 0.45; Figure 1F).

Chronic alterations in activity have also been shown to induce compensatory changes in intrinsic excitability (Desai et al., 1999). To assess whether cell-autonomous excitation can drive such changes, we measured action potential threshold in control and photostimulated neurons. Photostimulated neurons required greater depolarization to fire action potentials than control neurons (control: −27.9 ± 0.6 mV; n = 14; transfected: −24.2 ± 1.1 mV; n = 14; p < 0.001; Figure 1H). This result agrees with a recent study (Grubb and Burrone, 2010) that found that cell-autonomous excitation elicited a shift in axon initial segment position, which in turn correlates with action potential threshold. Input resistance, measured at −70 mV, was not significantly different between photostimulated and control neurons (Figure 1G). Together, these results demonstrate that neurons engage a precise and coordinated set of homeostatic changes in response to cell-autonomous excitation. For the remainder of the study we focused on compensatory synaptic changes.

We conducted several control experiments to determine whether nonspecific toxicity played any role in the synaptic depression. As noted above, input resistance in photostimulated neurons did not change (Figure 1G) arguing against deterioration of membrane integrity. Corroborating this result, photostimulated neurons did not show obvious morphological changes (Figure S1E). To see whether synaptic depression in photostimulated neurons was reversible, we illuminated ChR2-transfected neurons for 24 hr then allowed them to recover in the absence of light. Both AMPAR and NMDAR synaptic responses recovered after 4-7 days (Figure S1B). To check for nonspecific effects of fluorophore excitation on synaptic transmission, we illuminated GFP-expressing neurons with blue light for 48 hr. There was no change in synaptic transmission in GFP-expressing neurons relative to controls (Figure S1C). Compared to GFP, the mCherry ChR2 tag should be much less excited by blue light. Lastly, we checked for deterioration of neuron health downstream of light-induced depolarization by incubating neurons with an inhibitor of apoptosis, Bax inhibitor peptide V5 (Nikolaev et al., 2009). Photostimulation-induced synaptic depression was not affected by the inhibitor (Figure S1D). Altogether, these results argue against a role for nonspecific cell health deterioration in the synaptic depression.

Postsynaptic Expression Mechanism of Chronic Photostimulation-Induced Depression

The depression of AMPAR and NMDAR currents in chronically photostimulated neurons could be due to either pre- or postsynaptic changes. Since both AMPAR and NMDAR currents were reduced, a reduction in probability of release (P_r) could explain the parallel depression. Such a decrease in P_r would be accompanied by a corresponding increase in paired pulse ratio (PPR), which is inversely related to P_r (Manabe et al., 1993). However, no change in PPR between photostimulated and control neurons was observed (PPR transfected = 1.60 ± 0.1; PPR control = 1.58 ± 0.09; n = 15; p > 0.9; Figure 2A). As an additional measure of P_r, we compared the rate of decay of NMDAR responses between photostimulated and control neurons in the presence of the use-dependent NMDAR antagonist MK-801. Since MK-801 only blocks receptors that are opened by presynaptic neurotransmitter release, the rate of receptor blockade is proportional to P_r (Hessler et al., 1993). Similar to the results with PPR, however, there was no change in the rate of blockade of the NMDAR response between photostimulated and control neurons ($decay_{transfected}/decay_{control}$ = 1.21 ± 0.17; n = 10; p > 0.25; Figure 2B). These data argue against a change in P_r on photostimulated neurons.

Since there was no apparent change in P_r on photostimulated neurons, we investigated whether a change in quantal size or functional synapse number might explain the photostimulation-induced synaptic depression. We first recorded mEPSCs to test these possibilities. Photostimulated neurons had a small but significant reduction in quantal amplitude (control: 11.7 ± 0.5 pA; transfected: 9.6 ± 0.4 pA; n = 24; p < 0.0007; Figure 2C). More striking, however, was a large reduction in mEPSC frequency (Control: 0.25 ± 0.07 Hz; Transfected: 0.11 ± 0.01 Hz; n = 13; p < 0.05; Figure 2D). The large reduction in mEPSC frequency raised the possibility of a reduction of functional synapses, either due to synapse silencing by the complete loss of AMPARs or structural elimination. Consistent with these possibilities, photostimulated neurons exhibited a greater number of synaptic failures than control neurons in minimal stimulation experiments (failure rate control: 18.1 ± 4.7%; transfected: 31.0 ± 6.3%; n = 17; p < 0.035; Figure 2E). To distinguish between synapse silencing or structural elimination, we counted spines on Alexa-dye-filled neurons from photostimulated or non-photostimulated slices. We observed no change in spine density between transfected and control cells in nonphotostimulated conditions (control: 0.56 ± 0.08 spines μm^{-1}; transfected: 0.60 ± 0.12 spines μm^{-1}; n = 6; p > 0.8; Figure 2F). By contrast, in photostimulated slices spine density significantly decreased in

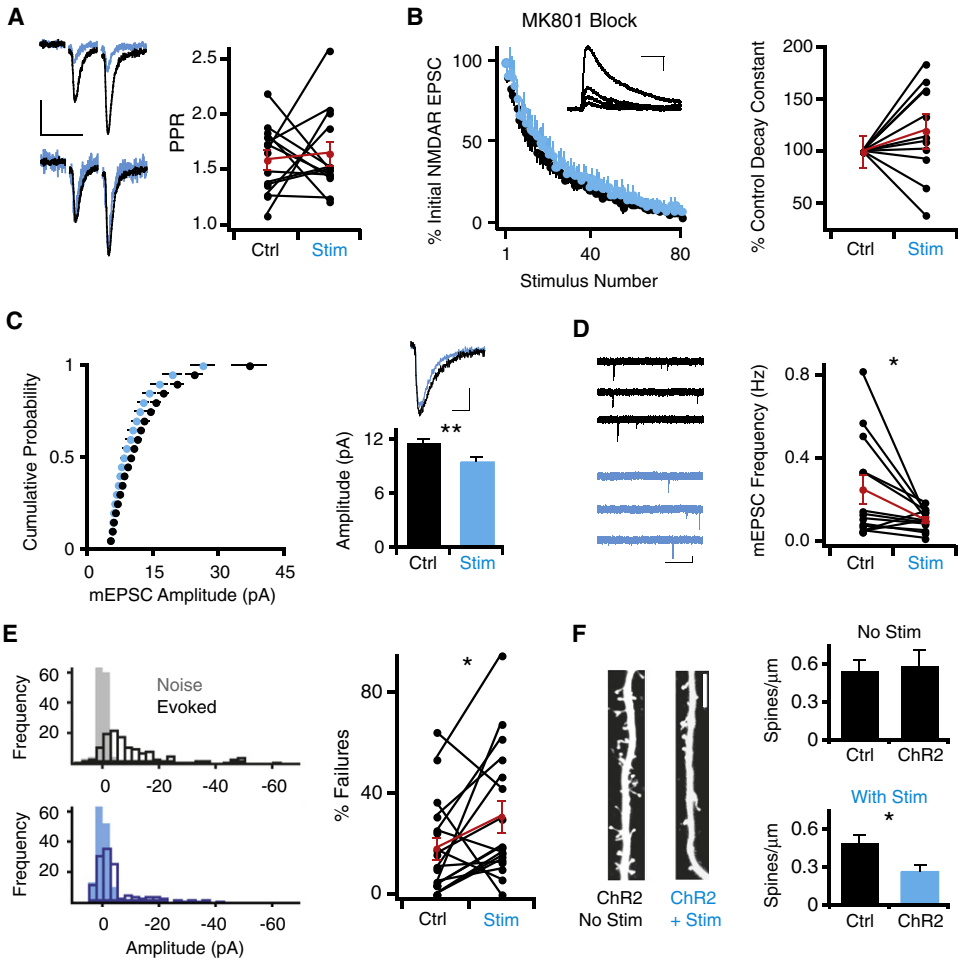

Figure 2. Photostimulation-Induced Synaptic Depression Involves Postsynaptic Synapse Elimination

(A) No significant difference in paired pulse ratio measured in ChR2-transfected and control neurons after 24 hr photostimulation. Left: Sample traces. Scale bar represents 50 ms, 15 pA.

(B) Plot of averaged NMDAR response amplitude, normalized to first response, versus stimulus number in the presence of the use-dependent irreversible NMDAR antagonist MK-801. Inset: representative traces showing progressive block of NMDAR currents in the presence of MK-801. Scale bar represents 100 ms, 25 pA. Right: Time constants for NMDAR current decay for each paired recording. Values for each pair are normalized to the control cell time constant. There was no significant change between ChR2-transfected and control neurons after photostimulation.

(C) Cumulative distribution of mEPSC amplitudes recorded in the presence of TTX. Right: Representative average mEPSC traces. Scale bar represents 10 ms, 3 pA; graph represents mean ± SEM mEPSC amplitudes. There is a small but significant decrease in mEPSC amplitude in ChR2-transfected photostimulated neurons.

(D) mEPSC frequency is significantly decreased in ChR2-transfected photostimulated neurons. Left: Representative traces. Scale bar represents 1 s, 10 pA.

(E) Synaptic failures measured during minimal stimulation experiments. Left: Representative histograms showing distributions of noise and post-stimulus amplitudes. Right: Quantification of synaptic failures in paired recordings; there is a significant increase in the number of synaptic failures in ChR2-transfected photostimulated neurons.

(F) Left: Example images of Alexa-dye filled apical dendrites of nonphotostimulated and photostimulated ChR2-transfected neurons. Scale bar represents 5 µm. Right, top: Quantification of primary apical dendrite spine density in pairs of neurons in nonphotostimulated slices. Right, bottom: Quantification of spine density in photostimulated slices. There is a significant decrease in spine density in ChR2-transfected neurons relative to control neurons in photostimulated slices.

ChR2-transfected neurons relative to control neurons (Control: 0.51 ± 0.05 spines μm^{-1}; transfected: 0.27 ± 0.05 spines μm^{-1}; n = 11; $p < 0.015$). These data suggest that the decrease in AMPAR and NMDAR synaptic currents in chronically photostimulated neurons could be due, at least in part, to the postsynaptic elimination of synapses; it is still possible, however, that some synapses are functionally silenced but structurally spared.

L-Type Voltage-Gated Calcium Channels Are Necessary for Photostimulation-Induced Depression

One possible explanation for the photostimulation-induced synaptic depression could be an NMDAR-dependent LTD-like effect; photostimulation might elevate NMDAR currents since photostimulation-evoked depolarization may facilitate NMDAR channel opening. Arguing against an LTD-like effect, however, bath applying the NMDAR antagonist D-APV (100 µM) during

the 24 hr photostimulation did not block the depression of AMPAR ($I_{transfected}/I_{control}$ = 0.40 ± 0.07; n = 18; $p < 10^{-4}$) or NMDAR currents ($I_{transfected}/I_{control}$ = 0.53 ± 0.16; n = 16; p < 0.02; Figures 3A and 3D). Similarly, blocking all excitatory transmission by bath applying both NBQX and APV during photostimulation did not impair the synaptic depression (Figures 3B and 3D). Finally, to test a requirement for pre- or postsynaptic action potentials, we bath applied the sodium channel antagonist TTX. TTX did not impair photostimulation-induced synaptic depression of either AMPARs or NMDARs (Figures 3C and 3D).

Since photostimulation-induced depression can be induced in the absence of synaptic activity or sodium channel activity, we next examined voltage-gated calcium channel function, since these channels should open during light-evoked depolarization. Bath application of low-dose nickel (100 μM), which selectively blocks R- and T-type calcium channels (Soong et al., 1993) did not impair the synaptic depression (Figure 4A), nor did bath application of ω-conotoxin GVIA (1 μM) (Figure 4B), an antagonist of N-type calcium channels (Tsien et al., 1988). In contrast, application of the L-type calcium channel antagonist nifedipine (20 μM) (Tsien et al., 1988) blocked the synaptic depression of AMPAR ($I_{transfected}/I_{control}$ = 1.07 ± 0.19; n = 20; p > 0.85) and NMDAR ($I_{transfected}/I_{control}$ = 0.77 ± 0.19; n = 17; p > 0.17) synaptic currents (Figures 4C and 4D). These data suggest that chronic heightened calcium influx through L-type calcium channels drives the synaptic depression. Although calcium flux through ChR2 cannot be detected by calcium imaging in CA1 pyramidal neurons (Zhang and Oertner, 2007), we cannot exclude the possibility that a small amount of calcium flux through the ChR2 channel itself may contribute to the process of synaptic depression (Nagel et al., 2003).

Photostimulation-Induced Depression Requires Transcription and Protein Translation

The long induction period required for photostimulation-induced synaptic depression (Figure S1) raises the possibility that protein translation or transcription might be altered. Indeed, treatment with the translational inhibitors cycloheximide (CXM) (100 μM) or anisomycin (ANS) (20 μM), or the transcriptional inhibitor 5,6-dichloro-1-β-D-ribobenzimidazole (DRB) (160 μM) blocked the depression of AMPAR synaptic currents in photostimulated neurons (CXM $I_{transfected}/I_{control}$ = 0.96 ± 0.18; n = 17; p > 0.75; ANS $I_{transfected}/I_{control}$ = 1.13 ± 0.26; n = 17; p > 0.2; DRB $I_{transfected}/I_{control}$ = 0.89 ± 0.22; n = 13; p > 0.85; Figures 5A and 5B). Surprisingly, neither cycloheximide nor DRB blocked the NMDAR depression (CXM $I_{transfected}/I_{control}$ = 0.53 ± 0.23; n = 11; p < 0.05; DRB $I_{transfected}/I_{control}$ = 0.46 ± 0.1; n = 13; p < 0.05). Spine density was not affected by DRB treatment, arguing against a nonspecific occlusion of synaptic depression (Figure S2). Since 24 hr inhibition of transcription or protein translation may reduce ChR2 expression level, we recorded from cells with high levels of ChR2 as visualized by the mCherry tag; measured light-evoked currents were similar across conditions (Figure 5C). Although up to this point our data are consistent with synapse elimination explaining the parallel depression of AMPAR and NMDAR function, the sensitivity of AMPAR depression but not NMDAR depression to cycloheximide or DRB treatment indicates that the phenomena are separable.

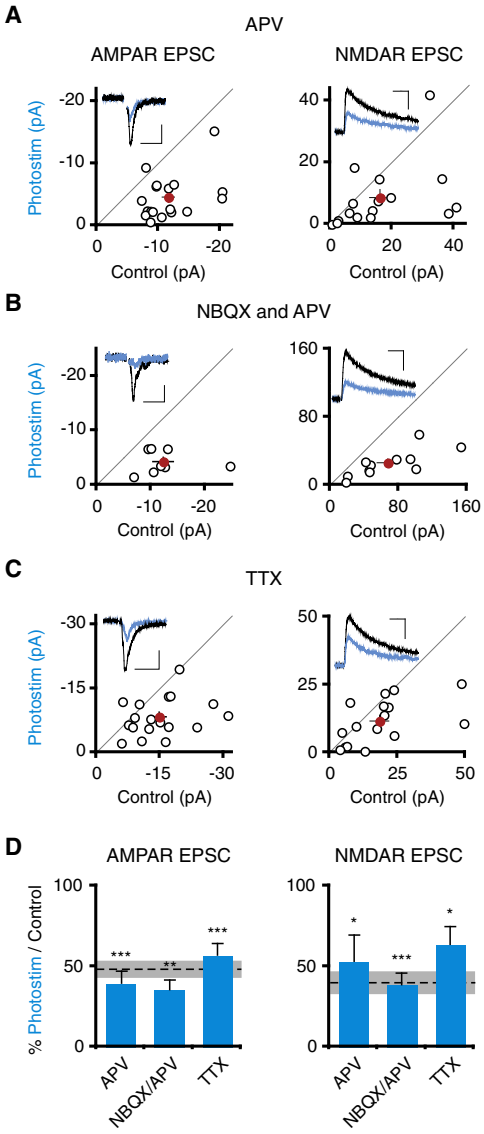

Figure 3. Synaptic Activity and Spiking Are Not Required for Photostimulation-Induced Synaptic Depression

(A) Slices were photostimulated for 24 hr in the presence of D-APV (100 μM). Scatter plots show AMPAR and NMDAR synaptic currents from ChR2-transfected and control cell pairs, as in Figure 1. AMPAR, NMDAR scale bars represent 50 ms, 5 pA; 100 ms, 20 pA.

(B) Same experiment as in (A) but including 50 μM D-APV and 20 μM NBQX in the slice media. Scale bars represent 50 ms, 5 pA; 100 ms, 100 pA.

(C) Same experiment as in (A) but including TTX (1 μM) in the slice media. Scale bars represent 50 ms, 10 pA; 100 ms, 30 pA.

(D) Summary graph of mean ± SEM EPSC amplitudes, expressed as a ratio of transfected to control neuron values. There was a significant depression of both AMPAR and NMDAR synaptic currents in ChR2-transfected photostimulated neurons in all three manipulations. Dashed lines/shaded area in this and subsequent figures represent mean ± SEM relative synaptic responses for photostimulated neurons in control conditions (repeated from Figure 1).

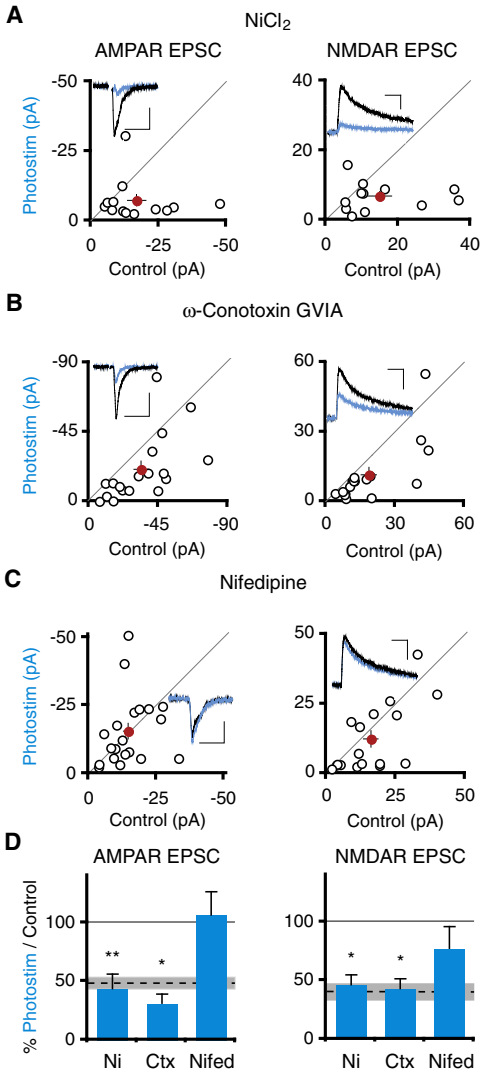

Figure 4. Activation of L-Type Voltage Gated Calcium Channels Is Required for Photostimulation-Induced Synaptic Depression

(A) Slices were photostimulated for 24 hr in the presence of nickel chloride (100 μM). Scatter plots show AMPAR and NMDAR synaptic currents from ChR2-transfected and control cell pairs. Scale bars represent 50 ms, 10 pA; 100 ms, 15 pA.

(B) Same experiment as in (A) but instead including ω-conotoxin GVIA (1 μM). Scale bars represent 50 ms, 20 pA; 100 ms, 20 pA.

(C) As in (A) but including nifedipine (20 μM). Scale bars represent 50 ms, 10 pA; 100 ms, 15 pA.

(D) Summary graph. Depression of AMPAR and NMDAR currents occurred in ChR2-transfected photostimulated neurons in the presence of nickel chloride or ω–conotoxin GVIA but not nifedipine.

The Role of the CaMKK/CaMK4 Pathway in Excitation-Induced Synaptic Depression

Cellular sensors are essential components of homeostatic systems (Davis, 2006), and so we explored candidate sensors that might detect the heightened influx of calcium during chronic photostimulation-induced depolarization. We tested inhibitors of several calcium-dependent kinases and phosphatases to investigate the involvement of their respective targets in the photostimulation-induced synaptic depression (Figure S3). Only the pan-CaMK inhibitor KN-93 prevented synaptic depression in photostimulated neurons.

The best known target of KN93, CaMKII, controls synaptic strengthening during LTP (Lisman et al., 2002; Wayman et al., 2008). At the *Drosophila* neuromuscular junction, CaMKII inhibition occludes the homeostatic response to decreased glutamate receptor function (Haghighi et al., 2003). In hippocampal neurons, alterations in neural activity shift the ratio of αCaMKII and βCaMKII isoforms, and this ratio shift has been implicated in the homeostatic response to activity suppression (Thiagarajan et al., 2002). We therefore tested whether blocking CaMKII inhibits photostimulation-induced synaptic depression by bath applying the CaMKII inhibitors myristoylated CaMKIINtide (myr-CaMKIIN, 10 μM) or myristoylated autocamtide-2 related inhibitory peptide (myr-AIP, 10 μM) during photostimulation (Chang et al., 1998; Ishida et al., 1995; Sanhueza et al., 2007). Neither inhibitor blocked the photostimulation-induced depression of AMPAR or NMDAR responses (Figures 6A–6C). Expression of CaMKIIN (4–6 days) or AIP (2–4 days) reduced synaptic AMPAR but not NMDAR responses in transfected neurons compared to control neurons (Figure 6E; W. Lu and R.A.N., unpublished data). Bath application of myristoylated-CaMKIIN for 1–2 days also decreased the ratio of synaptic AMPAR to NMDAR responses as compared to neurons in control media, demonstrating that myr-CaMKIIN penetrates cells (Figure 6D). This data also implies that photostimulation-induced depression is not limited by synaptic depression due to perturbation of independent molecular pathways.

Given the requirement for protein transcription in photostimulation-induced synaptic depression, we next explored the involvement of the CaMKK pathway because of its downstream target CaMK4, which regulates transcription (Wayman et al., 2008). Bath application of the CaMKK inhibitor STO-609 (3 μM) during chronic photostimulation blocked the synaptic depression of AMPAR ($I_{transfected}/I_{control}$ = 0.84 ± 0.10; n = 41; p > 0.15) and NMDAR synaptic currents ($I_{transfected}/I_{control}$ = 0.78 ± 0.10; n = 37; p > 0.15; Figures 7A and 7C). We confirmed that STO-609 specifically inhibits CaMKK in this process by coexpressing a STO-609 insensitive mutant CaMKKα, CaMKKL233F (Tokumitsu et al., 2003), in ChR2-transfected photostimulated neurons. CaMKKL233F coexpression restored photostimulation-induced synaptic depression in the presence of STO-609 (Figures 7B and 7C).

CaMKK phosphorylates and enhances the activities of CaMK1 and CaMK4 (Wayman et al., 2008). To determine the roles of these downstream kinases in photostimulation-induced synaptic depression, we coexpressed dominant negative constructs for each kinase (Wayman et al., 2006) in ChR2-transfected neurons. For each construct, we compared the effect on synaptic transmission of expressing the dominant-negative construct alone versus the combined effect of the construct and photostimulation. CaMK1DN-expressing cells exhibited a nonsignificant trend toward reduced AMPAR and NMDAR currents (Figure 7G). Photostimulation of CaMK1DN-expressing cells further depressed AMPAR and NMDAR currents (p < 0.05 AMPAR, p < 0.05 NMDAR, Mann-Whitney test, Figure 7G),

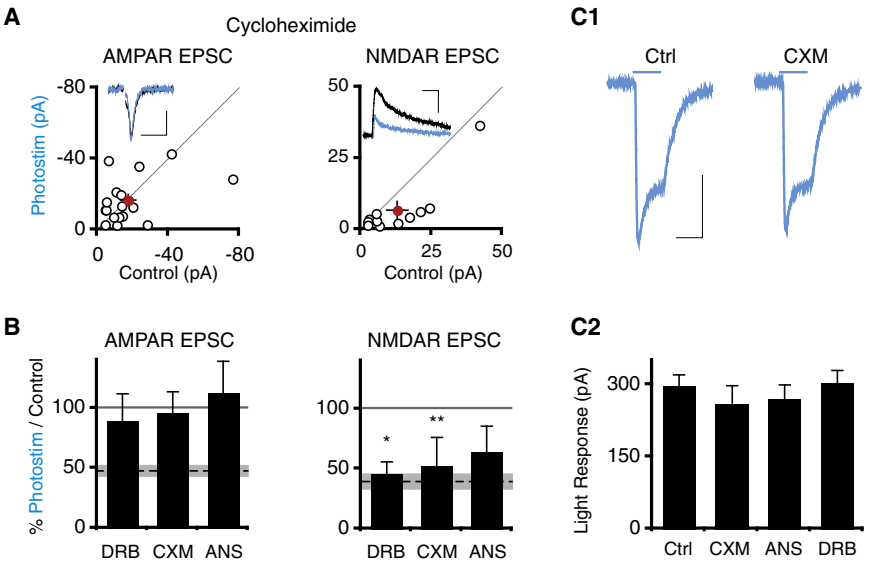

Figure 5. Transcription and Protein Translation Are Required for Photostimulation-Induced Synaptic Depression

(A) Scatter plots of synaptic currents from slices photostimulated 24 hr in the presence of cycloheximide (100 μM). Scale bars represent 50 ms, 20 pA; 100 ms, 15 pA.

(B) Summary graph of synaptic data from 5,6-dichloro 1-β D-ribobenzimidazole (DRB, 160 μM), cycloheximide (CXM), or anisomycin (ANS, 20 μM) treated slices.

(C) No decrease in ChR2 expression in recorded cells after drug treatments. C1: Representative traces of light pulse-evoked currents in non drug-treated ChR2-transfected neurons (synaptic current data in Figure 1) and cycloheximide-treated ChR2-transfected neurons. Scale bar represents 50 ms, 150 pA. C2: Graph shows mean ± SEM light pulse-evoked current in different conditions. See also Figure S2.

indicating that photostimulation-induced depression was intact. Cells expressing CaMK4DN had significantly reduced AMPAR and NMDAR synaptic currents. However, photostimulation of CaMK4DN-expressing cells did not further reduce AMPAR currents (CK4DN alone AMPAR $I_{transfected}/I_{control}$ = 0.59 ± 0.12; n = 22; CK4DN + Photostim $I_{transfected}/I_{control}$ = 0.56 ± 0.15; n = 13; p > 0.38 Mann-Whitney test; Figure 7G). The photostimulation-induced depression of NMDAR currents was also

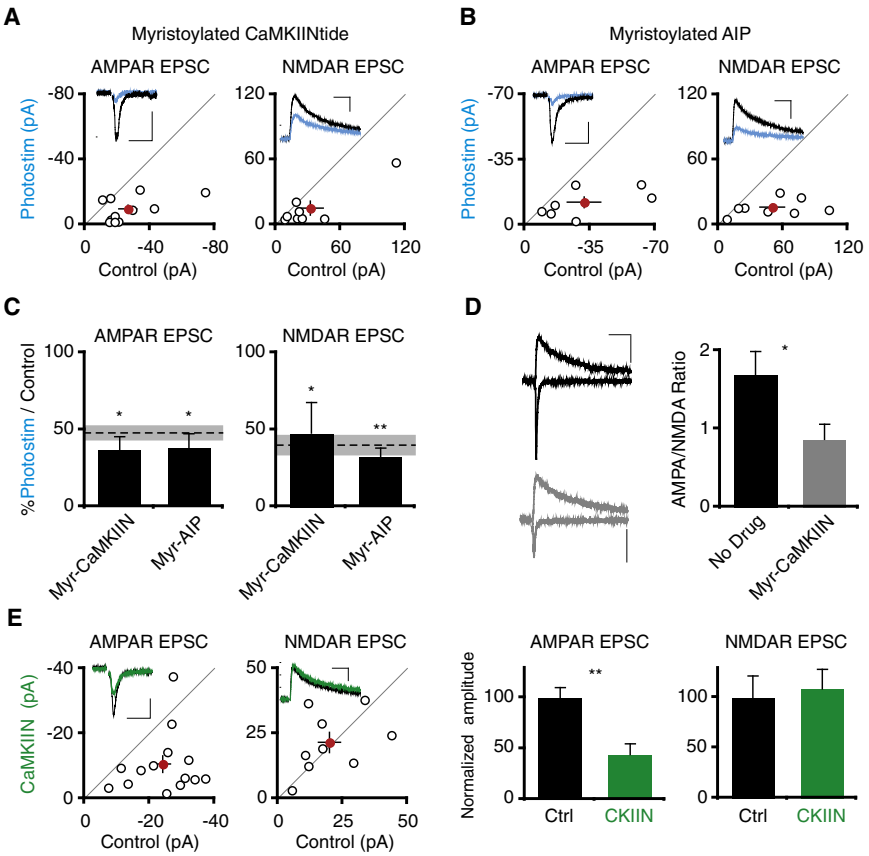

Figure 6. Inhibiting CaMKII Does Not Block Photostimulation-Induced Synaptic Depression

(A and B) Scatter plots showing data from slices photostimulated for 24 hr in the presence of myr-CaMKIIN or myr-autocamtide-2 related inhibitory peptide (myr-AIP). Scale bars represent (A) 50 ms, 10 pA; 100 ms; 50 pA. (B) 50 ms, 15 pA; 100 ms, 50 pA.

(C) Summary graph showing significant depression of both AMPAR and NMDAR responses by photostimulation in the presence of either myr-CaMKIIN or myr-AIP.

(D) Neurons treated with myristoylated-CaMKIIN (myr-CaMKIIN; 10 μM; 1–2 days) have decreased AMPA/NMDA ratios. Left: representative traces from control (top) or myr-CaMKIIN-treated (bottom) slices. Scale bar represents 50 ms, 10 pA.

(E) Synaptic responses from control- and EGFP-CaMKIIN-expressing neurons. Synaptic AMPAR responses are depressed in EGFP-CaMKIIN-expressing neurons. Scale bars represent 50 ms, 10 pA; 100 ms, 20 pA. See also Figure S3.

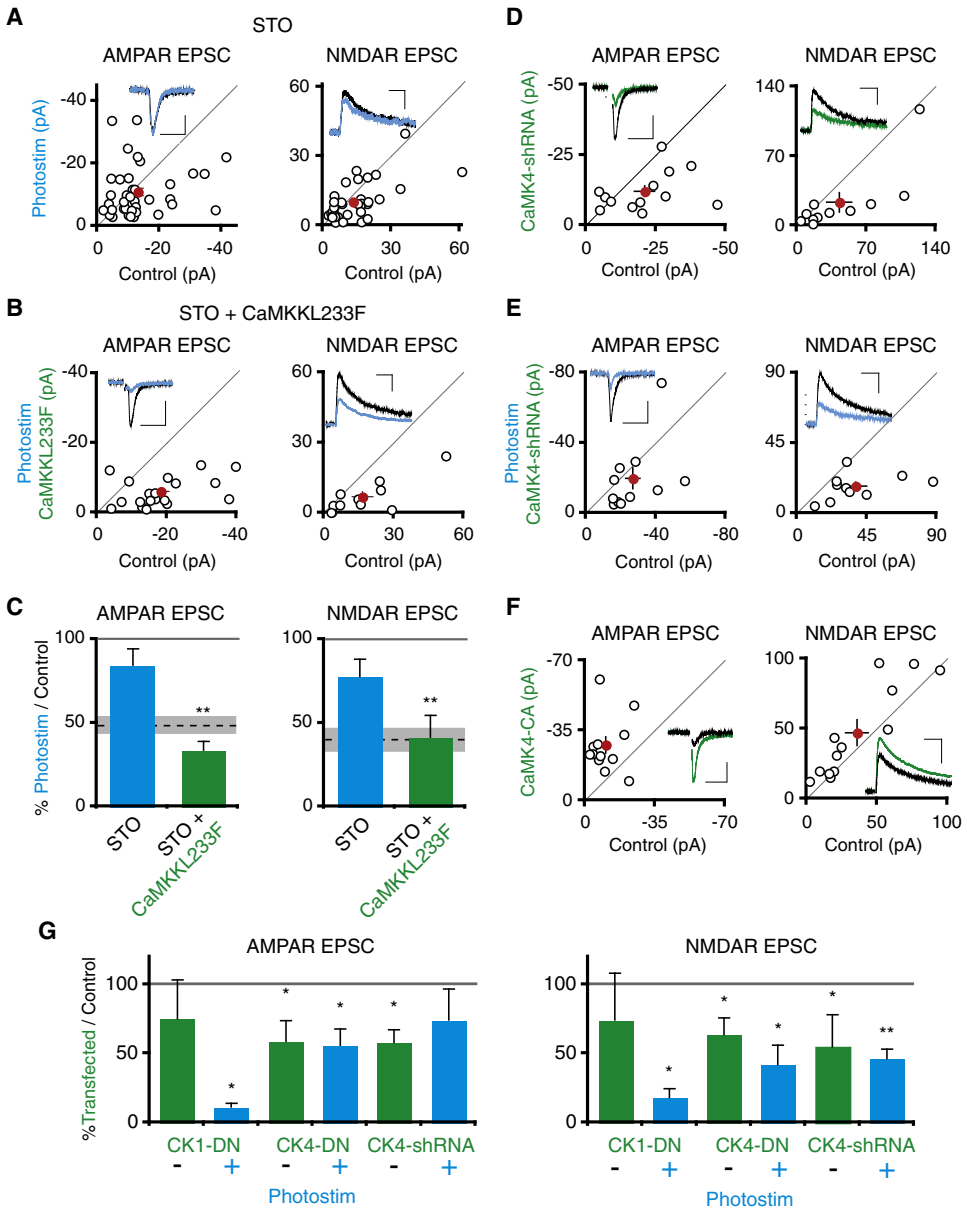

Figure 7. Activation of CaMKK and Its Downstream Target, CaMK4, Is Necessary for Photostimulation-Induced Synaptic Depression

(A) Slices were photostimulated for 24 hr in the presence of STO-609 (3 μM). Scatter plots show AMPAR and NMDAR synaptic currents from pairs of ChR2-transfected and control cell pairs. Scale bars represent 50 ms, 20 pA; 100 ms, 15 pA.

(B) Same as in (A), except ChR2-transfected cells were cotransfected with STO-609 resistant CaMKKL233F. Scale bars represent 50 ms, 20 pA; 100 ms, 25 pA.

(C) Summary graph. There is no significant depression of AMPAR and NMDAR synaptic currents in ChR2-transfected photostimulated neurons in the presence of STO-609, but there is a significant depression of AMPAR and NMDAR currents when ChR2-transfected photostimulated neurons are additionally transfected with CaMKKL233F.

(D) Scatter plot showing AMPAR and NMDAR synaptic currents from pairs of control neurons and neurons cotransfected with ChR2 and CaMK4-shRNA (not photostimulated). Scale bars represent 50 ms, 10 pA; 100 ms, 10 pA.

(E) Same as in (D) except neurons were photostimulated. Scale bars represent 50 ms, 20 pA; 100 ms, 20 pA.

(F) Scatter plot of synaptic responses from control neurons and neurons expressing constitutively active CaMK4 for 2 days. Scale bars represent 50 ms, 15 pA; 100 ms, 20 pA.

(G) Neurons were double-transfected with either ChR2 and dominant-negative CaMK1 or ChR2 and dominant-negative nuclear-localized CaMK4; paired recordings of transfected/control neuron pairs were conducted from either nonphotostimulated or photostimulated slices. Data from CaMK4-shRNA expressing neurons is also included. The relative amplitude of transfected/control neuron AMPAR or NMDAR synaptic currents in the different conditions is plotted. See also Figure S4.

impaired in CaMK4DN expressing cells (CK4DN alone NMDAR $I_{transfected}/I_{control}$ = 0.64 ± 0.12; n = 18 versus CK4DN + Photostim $I_{transfected}/I_{control}$ = 0.42 ± 0.14; n = 10; p > 0.56). Since dominant-negative kinases may have nonspecific effects, we also knocked down CaMK4 expression by expressing a CaMK4-shRNA construct (Ageta-Ishihara et al., 2009; Takemoto-Kimura et al., 2007). Similar to CaMK4DN, expression of CaMK4 shRNA depressed synaptic AMPAR and NMDAR responses (Figure 7D). This synaptic depression could be rescued by expression of shRNA-proof CaMK4 (Figure S4). However, as with dominant-negative CaMK4, photostimulation did not further depress AMPAR or NMDAR responses in neurons expressing CaMK4 shRNA (Figures 7E and 7G). These data indicate that activation of both CaMKK and its downstream target CaMK4 are required for photostimulation-induced synaptic depression.

In a simple model, activation of CaMK4 downstream of CaMKK activation in photostimulated neurons would trigger synaptic depression. Contrary to this prediction, 2 day expression of constitutively active CaMK4 (Enslen et al., 1996) potentiated synaptic AMPAR and NMDAR responses (Figure 7F), in agreement with previous results (Marie et al., 2005). We conclude that although CaMK4 is necessary for photostimulation-induced synaptic depression, it is not sufficient and instead is likely to act in concert with other factors.

Beyond CaMKK's role in photostimulation-induced synaptic depression, we next asked whether CaMKK also triggers synaptic depression in response to elevated synaptic activity. The STO-609 insensitive CaMKKL233F construct allows us to investigate the role of CaMKK activity in mediating any potential chronic synaptic-activity driven synaptic depression: by treating slices with STO-609, we can compare synaptic transmission between neurons in which CaMKK is blocked (control cells) and neurons in which CaMKK is spared (CaMKKL233F-expressing cells). Using this chemical genetic approach, we first assessed whether CaMKK regulates synaptic transmission in basal activity conditions. Synaptic transmission was unchanged between control neurons and neurons expressing STO-609 insensitive CaMKKL233F (Figure S5A). We then repeated this experiment but in the presence of STO-609 for 24 hr to block any CaMKK in control cells. Again there was no difference in synaptic responses between cells expressing the STO-609 resistant construct and neighboring cells exposed to STO-609 (Figure 8A). These data suggest that CaMKK does not regulate synaptic transmission in basal activity conditions in organotypic slices. We next assessed whether enhanced synaptic activity could drive CaMKK-mediated synaptic depression. We therefore increased synaptic activity by adding the $GABA_AR$ antagonist gabazine along with STO-609 to the slice media. After 24 hr of these elevated activity conditions, cells expressing STO-609 insensitive CaMKKL233F had significantly reduced AMPAR and NMDAR synaptic currents relative to control neurons (Figure 8B). The L-type calcium channel antagonist nifedipine blocked the synaptic depression of AMPAR ($I_{transfected}/I_{control}$ = 0.87 ± 0.19; n = 12; Figure 8C) and NMDAR responses ($I_{transfected}/I_{control}$ = 1.12 ± 0.19; n = 10) induced by elevated synaptic activity in CaMKKL233F-expressing neurons, consistent with the requirement for L-type calcium channel activity in photostimulation-induced synaptic depression. These experiments indicate that CaMKK is necessary for synaptic depression induced by chronically elevated synaptic activity. To see if the level of CaMKK activation is sufficient to determine the magnitude of chronic-activity induced synaptic depression, we overexpressed CaMKKL233F as before but treated slices with gabazine for 24 hr, excluding STO-609 (Figure 8D). In these conditions, synaptic AMPAR and NMDAR responses were diminished in cells overexpressing CaMKK relative to control neurons, suggesting that increasing CaMKK expression is sufficient to drive additional synaptic depression in response to elevated synaptic activity conditions.

We next conducted experiments to determine whether the downstream mechanisms of CaMKK activation in elevated synaptic activity conditions might share properties with the mechanisms of photostimulation-induced depression. mEPSC recordings from CaMKKL233F-expressing cells in slices treated with STO-609 and gabazine revealed a decrease in mEPSC frequency compared to control neurons (Figure S5C), similar to photostimulation-induced depression, although there was no change in mEPSC amplitude (Figure S5B). PPR did not change in CaMKKL233F-expressing neurons, also similar to photostimulation-induced depression and arguing against altered P_r (Figure S5D). Since gabazine treatment and photostimulation seem to share similar mechanisms, we wondered if they would cross-occlude. Gabazine treatment did not occlude further depression induced by photostimulation (Figure S5E), indicating that compensatory synaptic depression is not saturated when evoked either by elevated synaptic activity or photostimulation.

The GluA2 AMPAR Subunit Is Necessary for Shuttling AMPA Receptors Out of Photostimulation-Depressed Synapses

In a final set of experiments we began to investigate how the photostimulation-induced synaptic depression might be executed at the molecular level. Since specific subtypes of AMPARs are required for different types of synaptic plasticity (for example, GluA1 in LTP) (Bredt and Nicoll, 2003), we examined photostimulation-induced depression in mice lacking GluA1 or GluA2. In control slices from wild-type mice, photostimulation induced a depression of both AMPAR and NMDAR currents in ChR2-transfected neurons (AMPAR $I_{transfected}/I_{control}$ = 0.43 ± 0.09; n = 13; p < 0.004; NMDAR $I_{transfected}/I_{control}$ = 0.61 ± 0.20; n = 12; p < 0.01; Figures 9A and 9D), similar to that previously observed in rat slices (Figure 1D). Neurons from GluA1 deficient mice also undergo photostimulation-induced depression as normal (Figures 9B and 9D). By contrast, photostimulated neurons from GluA2 deficient mice do not undergo depression of AMPAR transmission ($I_{transfected}/I_{control}$ = 1.04 ± 0.15; n = 16; p > 0.55; Figures 9C and 9D). The photostimulation-induced depression of NMDAR responses remains intact in GluA2 knockout slices, however ($I_{transfected}/I_{control}$ = 0.64 ± 0.10; n = 12; p < 0.035), suggesting that the lack of GluA2 does not interfere with the mechanisms of photostimulation-induced synaptic depression upstream of AMPAR removal. Moreover, this result bolsters the conclusion from DRB or cycloheximide treatment data that independent pathways diverge downstream of CaMKK and CaMK4 activation to separately depress AMPAR and NMDAR function.

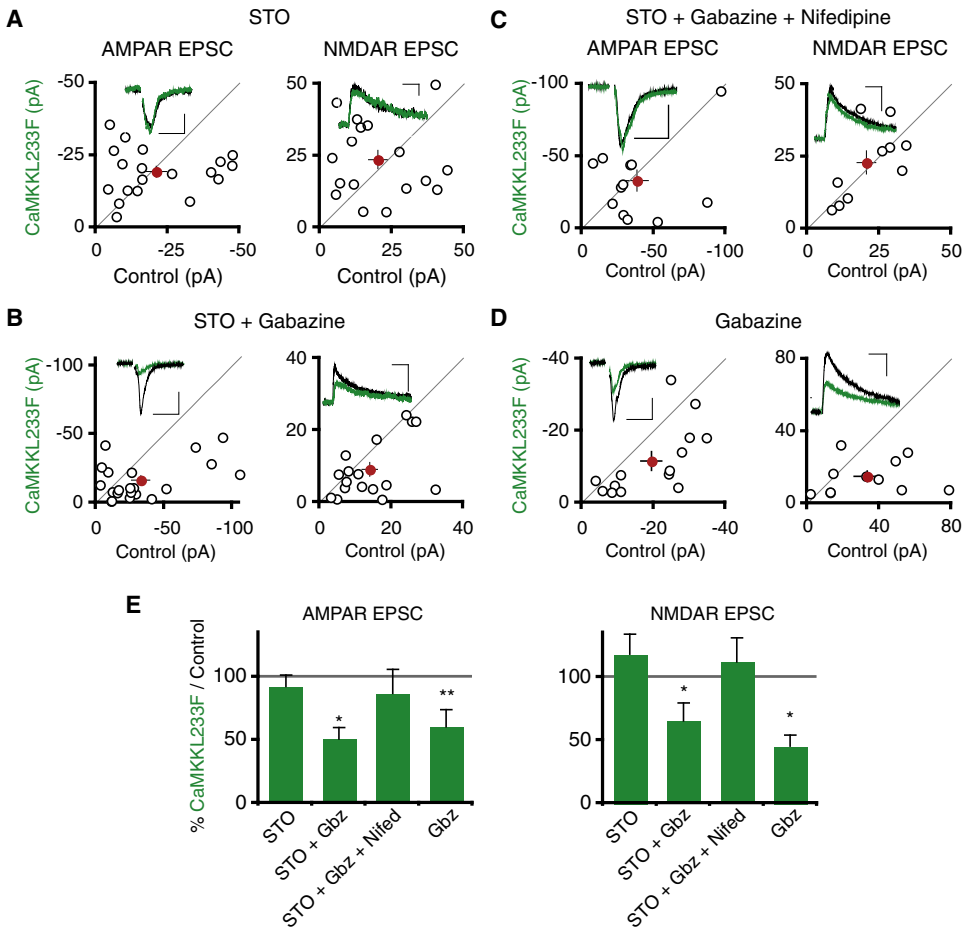

Figure 8. CaMKK Depresses Synaptic Transmission During Chronic Elevated Network Activity

(A) Scatter plot of synaptic currents from pairs of CaMKKL233F-transfected versus control neurons treated for 24 hr with STO-609 (3 μM). Scale bars represent 50 ms, 5 pA; 100 ms, 10 pA.

(B) Same as in (A) except slices were treated for 24 hr with both STO-609 and gabazine (10 μM). Scale bars represent 50 ms, 25 pA; 100 ms, 15 pA.

(C) Same as in (A) except slices were treated with STO-609, gabazine, and nifedipine (20 μM). Scale bars represent 50 ms, 15 pA; 100 ms, 20 pA.

(D) Same as in (A) except slices were treated with gabazine alone. Scale bars represent 50 ms, 10 pA; 100 ms, 30 pA.

(E) Summary graph. See also Figure S5.

One possible explanation for the absence of depression of synaptic AMPAR responses in GluA2-lacking neurons could be that the mechanism of photostimulation-induced depression requires selective removal of GluA2-containing AMPARs from synapses. We therefore assayed the composition of synaptic AMPARs remaining after photostimulation-induced depression by measuring synaptic rectification; if the remaining receptors lacked GluA2, we would expect those synapses to be rectifying. Synaptic rectification was unaffected by photostimulation, however (control rectification index: 0.87 ± 0.03; n = 7; photostim: 0.87 ± 0.18; n = 7; Figure 9E), indicating no change in the GluA2 composition of the remaining synaptic AMPARs.

Finally, we wondered whether all surface AMPARs are internalized in photostimulation-induced depression, or whether synaptic AMPARs are selectively removed. To investigate what happens to extrasynaptic AMPARs, we measured AMPAR currents in somatic outside-out patches from photostimulated and control neurons. Glutamate evoked currents were actually enhanced in patches from photostimulated neurons (Figure 9F), ruling out the possibility that all AMPARs were uniformly internalized from the cell surface. Instead, this result suggests that synaptic AMPARs may be shuffled to extrasynaptic membranes during photostimulation-induced depression.

DISCUSSION

Network-wide increases in activity can trigger homeostatic plasticity (O'Brien et al., 1998; Thiagarajan et al., 2005; Turrigiano et al., 1998). However, it is unknown whether neurons can homeostatically adjust synaptic strength in response to cell-autonomous increases in activity. By using photostimulation to cell-autonomously excite ChR2-transfected CA1 pyramidal neurons, we demonstrated a compensatory postsynaptic depression of AMPAR- and NMDAR-mediated synaptic transmission. Surprisingly, there is no compensatory increase in inhibitory currents. The compensatory synaptic depression of AMPARs

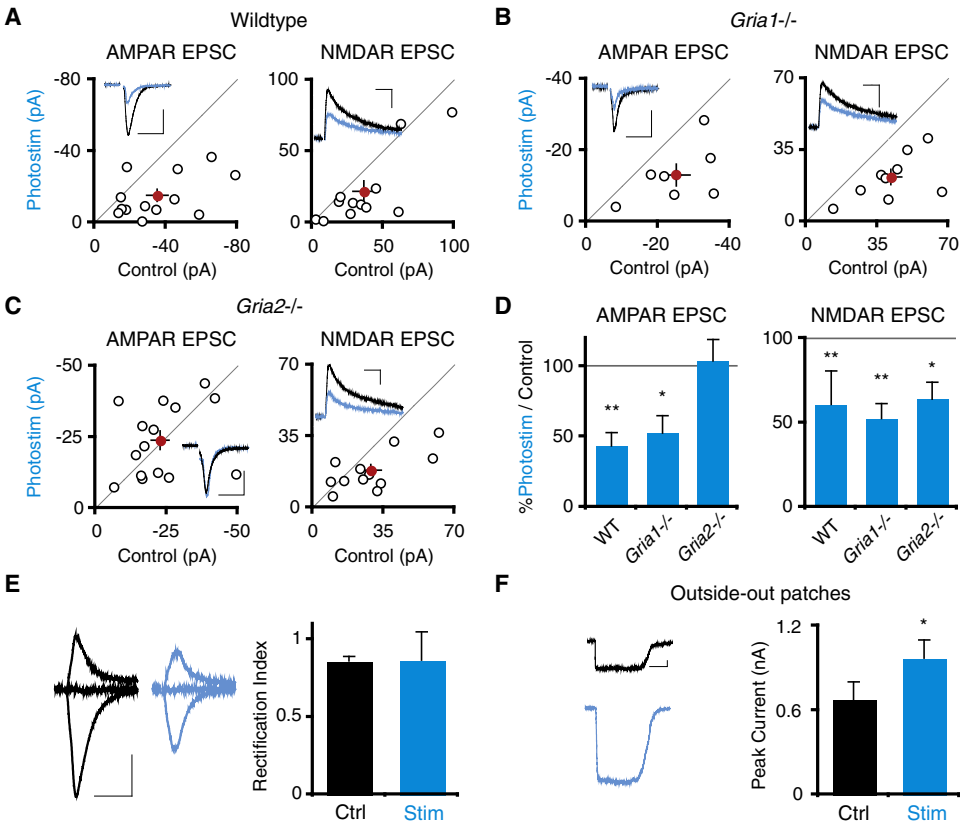

Figure 9. Photostimulation-Induced Synaptic Depression Requires the GluA2 AMPAR Subunit

(A–C) Scatter plots show AMPAR and NMDAR synaptic currents from pairs of ChR2-transfected versus control neurons photostimulated 24 hr, from wild-type, GluA1 (*gria1)* knockout, and GluA2 (*gria2*) knockout mice, respectively. There is a significant depression of synaptic currents for photostimulated versus control cells in all conditions except AMPAR responses in the GluA2 knockout. Scale bars represent (A) 50 ms, 40 pA; 100 ms, 25 pA; (B) 50 ms, 20 pA; 100 ms, 30 pA; (C) 50 ms, 20 pA; 100 ms, 30 pA.

(D) Summary graph of data in (A–C).

(E) Left: AMPAR responses measured in the presence of D-APV at −70, 0 and +40 mV in control and photostimulated neurons. Scale bar represents 50 ms, 50 pA. There is no significant change in rectification index, the ratio of responses at +40 mV and −70 mV, between control and ChR2-transfected, photostimulated neurons.

(F) Glutamate-evoked AMPAR currents in somatic outside-out patches from control and ChR2-transfected, photostimulated neurons. There is a significant increase in current amplitude in patches from ChR2-transfected neurons. Scale bar represents 1 s, 100 pA.

and NMDARs requires L-type voltage gated calcium channel activity but does not depend on excitatory synaptic activity or sodium spikes, indicating that the homeostatic depression is solely sensitive to the calcium influx downstream of membrane depolarization. Using molecular and pharmacological manipulations, we found that compensatory synaptic depression requires CaMKK activation of CaMK4. Downstream of CaMKK and CaMK4 activation independent pathways control AMPAR removal and NMDAR removal; AMPAR but not NMDAR removal requires transcription and protein synthesis, and AMPAR removal specifically requires the GluA2 AMPAR subunit.

Chronic photostimulation of ChR2-transfected neurons in organotypic slices offers several advantages over previous approaches to the study of homeostatic plasticity in central neurons. First, cell autonomous stimulation should avoid release of the potentially complex cocktail of signals that is triggered by perturbations of network activity states (Aoto et al., 2008; Stellwagen and Malenka, 2006). Second, the use of photostimulation permits precise control over the strength and duration of neural activity. Third, the use of paired whole-cell recordings in organotypic slices rigorously controls for slice-to-slice variability and allows direct measurements of synaptic transmission.

Cell-Autonomous Induction and Expression of Compensatory Synaptic Depression in Pyramidal Neurons

Our data show that activation of homeostatic sensors in individual neurons is sufficient to generate a compensatory response to elevated activity. Photostimulation initiated compensatory synaptic depression even when network-wide synaptic activity or spiking was blocked (Figure 3), indicating that neither simultaneous activation of other cell types nor local synaptic activity were required. Together with previous studies demonstrating that suppression of activity in individual neurons

induces compensatory changes in synaptic strength (Burrone et al., 2002; Ibata et al., 2008), or that cell-autonomous perturbations in activity modify intrinsic excitability (Turrigiano et al., 1994; Grubb and Burrone, 2010), we conclude that cell-autonomous sensors bidirectionally detect activity perturbations and initiate compensatory responses. In the brain, a cell-autonomous homeostatic mechanism has the advantage of curtailing hyperactivity of individual neurons prior to the generation of pathological network-wide hyperactivity. Although network-wide enhancement of activity triggers homeostatic changes in synaptic inhibition (Otis et al., 1994; Wierenga and Wadman, 1999), the compensatory synaptic modifications resulting from cell-autonomous elevated activity are limited to depression of excitatory synaptic function, since synaptic inhibition does not change after 24 hr of cell-autonomous excitation (Figure 1). Similarly, cell-autonomous suppression of activity does not alter GABA transmission (Hartman et al., 2006). Intercellular signals between neurons or between nonneural cell types and neurons may instead direct homeostatic adjustment of inhibitory synapses.

Although cell-autonomous excitation is sufficient to elicit synaptic homeostasis in CA1 pyramidal neurons, we cannot exclude a requirement for developmental or permissive signaling from glia or other cell types (Stellwagen and Malenka, 2006; Goold and Davis, 2007). Additionally, although the homeostatic sensor is cell-autonomous it remains possible that neurons emit signals that act locally to depress postsynaptic function. Diffusible retinoic acid has been proposed to play such a role in homeostatic responses to activity blockade (Aoto et al., 2008).

Our data argue that the expression site of compensatory synaptic depression is postsynaptic. Using two measures of presynaptic release, no presynaptic changes were found in chronically excited neurons (Figure 2; Figure S5). As further evidence against presynaptic changes, the photostimulation-induced depression of NMDAR responses can occur independently of an AMPAR depression (Figures 5 and 9). Thus, both the induction and expression site for compensatory synaptic depression are contained in the postsynaptic neuron. Although we found no evidence of retrograde modulation of presynaptic release on to photostimulated neurons, it is equally possible that the outputs of photostimulated neurons are regulated by elevated activity. The decrease in excitability that we (Figure 1) and others (Grubb and Burrone, 2010) observe in response to cell-autonomous excitation might combine with compensatory alterations in presynaptic release in the excited neuron to ensure that excess activity does not propagate through the brain. Homeostatic regulation of the synaptic outputs of a neuron might contribute to the observed compensatory modifications of presynaptic properties of excitatory synapses in response to network-wide perturbations of activity (Branco et al., 2008; Murthy et al., 2001; Thiagarajan et al., 2005).

The prevailing model of synaptic homeostasis, predominantly derived from studies of cortical neurons, holds that multiplicative synaptic scaling globally modifies synaptic strength to preserve information that is hypothesized to be stored in relative synaptic weights (Turrigiano, 2008). However, the majority of the photostimulation-induced synaptic depression we observe in CA1 pyramidal neurons, either elicited via photostimulation (Figure 2) or gabazine treatment of CaMKK-rescued neurons (Figure 8), can be attributed primarily to reduced synapse number, not synaptic strength. This finding is consistent with a study in vivo on hippocampal neurons demonstrating increased spine number after chronic suppression of activity (Kirov and Harris, 1999) (and see below discussion on changes in epileptic hippocampus).

The Homeostatic Signal in CA1 Neurons

In homeostatic systems, deviations in activity from a "set point" optimal level of activity lead to activation of sensors that initiate compensatory changes (Davis, 2006). We and others (Thiagarajan et al., 2005) identify L-type calcium channel activity as a proxy for activity that activates sensors in synaptic homeostasis. More specifically, our data suggest that the integrated sum of somatic depolarization, in the form of L-type calcium channel activity, governs compensatory synaptic depression. Spike activity is not required, since TTX did not block compensatory synaptic depression. We also found no evidence that local synaptic depolarization or calcium influx is necessary for compensatory synaptic depression, since blockade of either NMDARs or AMPARs did not block the depression. There was a nonsignificant trend toward increased photostimulation-induced depression in NBQX and APV treated slices, suggesting that a potentially exacerbated difference in activity between control and photostimulated neurons evoked a larger depression in photostimulated neurons. However, these data should be viewed with some caution, since a fraction of the decrease in transmission in photostimulated neurons might in principle result from reversal of any synaptic upregulation induced by activity blockade. In contrast, blockade of L-type calcium channel activity prevented the compensatory synaptic depression that was induced either by photostimulation (Figure 4) or by elevated synaptic activity (Figure 8). L-type channels are well suited to integrate somatic depolarization because of their graded activation near resting membrane potentials, slow inactivation kinetics, and high levels of expression in the soma and proximal apical dendrites (Magee et al., 1996; Westenbroek et al., 1990).

CaM Kinases and Synaptic Homeostasis

During neural activity, calcium binds calmodulin, which in turn activates CaM kinases (Wayman et al., 2008). Local synaptic calcium influx is thought to trigger synaptic strengthening through activation of CaMKII and other kinases (Lisman et al., 2002). Our data (Figure 6) and other studies (Sanhueza et al., 2007) further indicate that CaMKII activity is essential for normal synaptic strength. Although activity modifies the differential expression of CaMKII isoforms, which in turn regulates CaMKII properties (Thiagarajan et al., 2002), selective inhibition of CaMKII did not interfere with photostimulation-induced depression (Figure 6). This suggests that, during chronic cell-autonomous excitation, CaMKII functions independently of global homeostatic sensors.

To explain the homeostatic synaptic depression due to chronic calcium influx, our results instead delineate a molecular pathway that begins with calcium influx activating CaMKK, which in turn activates CaMK4 and other factors. Thus, CaMKK and CaMK4 appear to be components of a homeostatic sensor in pyramidal neurons. In support of this conclusion, the CaMKK

inhibitor STO-609 impairs photostimulation-induced synaptic depression; the synaptic depression can be restored by expression of a STO-609 insensitive CaMKK (Figure 7). Similarly, in conditions of network-wide elevated synaptic activity there is a CaMKK-dependent compensatory postsynaptic depression of AMPAR and NMDAR function (Figure 8). We identified CaMK4 as a target of CaMKK in compensatory synaptic depression, since expression of either shRNA against CaMK4 or dominant-negative CaMK4, but not dominant-negative CaMK1, blocked photostimulation-induced synaptic depression. CaMKK and CaMK4 have been shown to be necessary for synaptic scaling in response to inhibition of activity in dissociated neocortical neurons, and inhibition of CaMKK with STO-609 was reported to increase mEPSC amplitude in dissociated cortical neurons (Ibata et al., 2008). Taken together with our demonstration of a block of compensatory synaptic depression by DN-CaMK4, these results suggest CaMKK and CaMK4 are capable of bidirectionally controlling homeostatic plasticity. However, in our experimental system, we did not observe changes in synaptic function upon inhibiting CaMKK in basal conditions (Figure 8). One possibility is that CaMKK remains quiescent in basal conditions in organotypic slices.

Although our data suggest that levels of CaMKK activation control the magnitude of compensatory synaptic depression, the same is not true for CaMK4. After 24 hr of elevated network activity, neurons overexpressing CaMKK have reduced synaptic transmission relative to control neurons (Figure 8). This result suggests that the degree of CaMKK activation directly controls compensatory synaptic depression. If CaMK4 were similarly sufficient for compensatory synaptic depression, CaMK4 activation on its own should depress synaptic transmission. By contrast, expression of constitutively active CaMK4 enhances AMPAR and NMDAR currents (Figure 7) (Marie et al., 2005). These data suggest that CaMKK activates both CaMK4 and other, unknown factors to drive compensatory homeostatic depression, and that these downstream targets must act together to mediate compensatory homeostatic depression. CaMKK/CaMK4 activation has been implicated in late-phase LTP (Wayman et al., 2008). In response to the calcium influx induced by LTP protocols, CaMK4 activation may thus help maintain local strengthening of synapses. During conditions of chronic global calcium influx, CaMKK seems to activate both CaMK4 and other factors that together control global downregulation of synapses. It remains to be determined how the temporal structure, spatial extent, or magnitude of calcium influx might differentially regulate the action of CaMKK and its downstream targets.

CaMK4 and other effectors modulate the expression of numerous genes in response to L-type calcium channel activation (Dolmetsch et al., 2001; Murphy et al., 1991; Wayman et al., 2008). Consistent with a role for transcription in compensatory depression, a long (24 hr) induction period was required (Figure S1), and pharmacological inhibition of transcription or translation blocked the AMPAR component of synaptic depression (Figure 5). This suggests that photostimulation induces transcription and translation of molecules that execute the compensatory synaptic depression of AMPAR responses, such as Plk2/serum-inducible kinase (Seeburg et al., 2008). It is less clear which transcription factors might play a role in compensatory synaptic depression. The best known target of CaMK4, the transcription factor CREB, is thought to be activated by a combination of transient CaMK4 signaling and slower Ras-MAPK signaling (Wu et al., 2001). However, inhibitors of MAPK signaling did not block photostimulation-induced depression (Figure S3). This result suggests either that sustained CaMK4 activation evoked by photostimulation permits CaMK4 to maintain CREB activation on its own, or that other CaMK4-modulated transcriptional regulators mediate photostimulation-induced depression.

Parallel but Independent Homeostatic Regulation of AMPAR and NMDAR Function

Although compensatory synaptic depression induces simultaneous spine elimination, AMPAR depression and NMDAR depression, these processes can be dissociated in GluA2 knockout mice and conditions of transcription or protein synthesis inhibition. Two conclusions can be drawn from these results. First, synapse elimination is not upstream of AMPAR and NMDAR depression, since synapse elimination would be expected to simultaneously depress both AMPAR and NMDAR responses. Second, although L-type channel activation, CaMKK function and CaMK4 function are all required for both AMPAR and NMDAR depression, molecular pathways diverge downstream of these processes to regulate AMPAR and NMDAR removal. The necessity of GluA2 but not GluA1 for AMPAR compensatory synaptic depression (Figure 9) suggests that proteins selectively binding GluA2 but not GluA1 or NMDARs, such as GRIP, PICK1, or NSF are likely to mediate the removal of AMPARs from the synapse during homeostatic plasticity (Bredt and Nicoll, 2003; Song and Huganir, 2002). GluA2 knockdown also blocks the synaptic scaling up that occurs in response to inhibition of activity in dissociated culture (Gainey et al., 2009), suggesting a bidirectional homeostatic role for a molecular pathway involving GluA2 and its partners. Although the calcium permeability of GluA2-lacking AMPARs might alter basal calcium levels in GluA2 knockout mice, it should be noted that GluA2 knockout mice express normal hippocampal LTD and LTP (Meng et al., 2003). Therefore, the block of homeostatic plasticity in these mice cannot be explained by a general defect in plasticity.

AMPAR transmission contributes the majority of excitatory drive to pyramidal neurons, and compensatory AMPAR depression might be expected to reduce excess neural firing. The function of NMDAR depression is less obvious. Since NMDARs are blocked by Mg^{2+} at resting membrane potentials, NMDARs have traditionally been viewed as detectors of coincident pre- and postsynaptic activity that gate plasticity and functional synapse development (Bredt and Nicoll, 2003). Beyond plasticity, however, NMDAR EPSPs facilitate during repetitive stimulation (Cash and Yuste, 1999) and boost larger single EPSPs (Schiller et al., 2000). Thus, NMDAR depression may contribute to weakening excitatory drive after photostimulation-induced depression.

Homeostatic Synapse Elimination in Epilepsy

Pathological conditions of excess activity might be expected to trigger homeostatic processes. A reduction in spine density has been widely documented in human temporal lobe epilepsy (Isokawa et al., 1997; Scheibel et al., 1974) yet little is known

about the molecular mechanisms underlying this decrease in spine density or whether it involves intercellular or intracellular signaling (Swann et al., 2000). In light of the results presented here, it is tempting to speculate that a cell-autonomous compensatory response to chronic excitation explains the spine loss observed in epileptic brains.

EXPERIMENTAL PROCEDURES

Slice Culture and Photostimulation

Organotypic hippocampal slice cultures were prepared from P6-8 rats or mice, as described in the Supplemental Experimental Procedures. Slices were biolistically transfected with DNA constructs after 2–3 days in vitro (DIV) and recorded after 6–10 DIV. For photostimulation, 8–12 slices were consolidated on a culture plate insert and illuminated with a collimated blue light-emitting diode (470 nm) (Thorlabs). Manufacturer lists total beam power as 195 mW, beam area 1963 mm^2.

Electrophysiology

Simultaneous dual whole-cell recordings and data analysis were performed as described in the Supplemental Experimental Procedures. Briefly, AMPAR and NMDAR EPSCs were isolated with 100 μM picrotoxin and 10 μM gabazine. TTX (0.5–1 μM) was added to isolate mEPSCs. For MK-801 NMDAR decay experiments, solution containing 40 μM MK-801 was perfused over the slice for 5–10 min while cells were held at −70 mV. For rectification experiments cells were recorded in 100 μM D-APV and GABAR blockers. Rectification index was calculated according to the formula: $((I_{+40\ mV} - I_{0\ mV})/40)/((I_{0\ mV} - I_{-70\ mV})/70)$, where I = AMPAR current. ChR2 expression level (Figure 5) was measured using pulses of light by gating mercury arc lamp fluorescence through a 40× objective with a Uniblitz shutter or by manually engaging blue filter. Photocurrents were measured >50 ms after light onset.

Anatomy and Imaging

Pairs of control and ChR2-expressing cells in the same slice were filled with intracellular solution containing Alexa Fluor 488 for 5–10 min, then fixed and imaged. For experiments in Figure S1 and Figure S2, cells were cotransfected with ChR2 and EGFP; slices were fixed and immunostained.

SUPPLEMENTAL INFORMATION

Supplemental Information includes Supplemental Experimental Procedures and five figures and can be found with this article online at doi:10.1016/j.neuron.2010.09.020.

ACKNOWLEDGMENTS

We are grateful to K. Deisseroth for ChR2 constructs, T. Soderling for CaMK constructs, and to M. Nonaka and H. Bito for CaMK4 shRNA reagents. We thank K. Bjorgan and P. Apostolides for technical assistance, and G. Davis, A. Jackson, J. Levy, W. Lu, and S. Shipman for comments on the manuscript. C.P.G. was supported by a NSF predoctoral fellowship. R.A.N. is supported by grants from the National Institute of Mental Health.

Accepted: August 16, 2010
Published: November 3, 2010

REFERENCES

Ageta-Ishihara, N., Takemoto-Kimura, S., Nonaka, M., Adachi-Morishima, A., Suzuki, K., Kamijo, S., Fujii, H., Mano, T., Blaeser, F., Chatila, T.A., et al. (2009). Control of cortical axon elongation by a GABA-driven Ca2+/Calmodulin-dependent protein kinase cascade. J. Neurosci. *29*, 13720–13729.

Ahmed, O.J., and Mehta, M.R. (2009). The hippocampal rate code: Anatomy, physiology and theory. Trends Neurosci. *32*, 329–338.

Aoto, J., Nam, C.I., Poon, M.M., Ting, P., and Chen, L. (2008). Synaptic signaling by all-trans retinoic acid in homeostatic synaptic plasticity. Neuron *60*, 308–320.

Bellone, C., and Nicoll, R.A. (2007). Rapid bidirectional switching of synaptic NMDA receptors. Neuron *55*, 779–785.

Boyden, E.S., Zhang, F., Bamberg, E., Nagel, G., and Deisseroth, K. (2005). Millisecond-timescale, genetically targeted optical control of neural activity. Nat. Neurosci. *8*, 1263–1268.

Branco, T., Staras, K., Darcy, K.J., and Goda, Y. (2008). Local dendritic activity sets release probability at hippocampal synapses. Neuron *59*, 475–485.

Bredt, D.S., and Nicoll, R.A. (2003). AMPA receptor trafficking at excitatory synapses. Neuron *40*, 361–379.

Burrone, J., and Murthy, V.N. (2003). Synaptic gain control and homeostasis. Curr. Opin. Neurobiol. *13*, 560–567.

Burrone, J., O'Byrne, M., and Murthy, V.N. (2002). Multiple forms of synaptic plasticity triggered by selective suppression of activity in individual neurons. Nature *420*, 414–418.

Buzsaki, G., Csicsvari, J., Dragoi, G., Harris, K., Henze, D., and Hirase, H. (2002). Homeostatic maintenance of neuronal excitability by burst discharges in vivo. Cereb. Cortex *12*, 893–899.

Caeser, M., and Aertsen, A. (1991). Morphological organization of rat hippocampal slice cultures. J. Comp. Neurol. *307*, 87–106.

Cash, S., and Yuste, R. (1999). Linear summation of excitatory inputs by CA1 pyramidal neurons. Neuron *22*, 383–394.

Chang, B.H., Mukherji, S., and Soderling, T.R. (1998). Characterization of a calmodulin kinase II inhibitor protein in brain. Proc. Natl. Acad. Sci. USA *95*, 10890–10895.

Davis, G.W. (2006). Homeostatic control of neural activity: From phenomenology to molecular design. Annu. Rev. Neurosci. *29*, 307–323.

Desai, N.S., Rutherford, L.C., and Turrigiano, G.G. (1999). Plasticity in the intrinsic excitability of cortical pyramidal neurons. Nat. Neurosci. *2*, 515–520.

Dickman, D.K., and Davis, G.W. (2009). The schizophrenia susceptibility gene dysbindin controls synaptic homeostasis. Science *326*, 1127–1130.

Dolmetsch, R.E., Pajvani, U., Fife, K., Spotts, J.M., and Greenberg, M.E. (2001). Signaling to the nucleus by an L-type calcium channel-calmodulin complex through the MAP kinase pathway. Science *294*, 333–339.

Enslen, H., Tokumitsu, H., Stork, P.J.S., Davis, R.J., and Soderling, T.R. (1996). Regulation of mitogen-activated protein kinases by a calcium/calmodulin-dependent protein kinase cascade. Proc. Natl. Acad. Sci. USA *93*, 10803–10808.

Frank, C.A., Kennedy, M.J., Goold, C.P., Marek, K.W., and Davis, G.W. (2006). Mechanisms underlying the rapid induction and sustained expression of synaptic homeostasis. Neuron *52*, 663–677.

Frank, C.A., Pielage, J., and Davis, G.W. (2009). A presynaptic homeostatic signaling system composed of the Eph receptor, ephexin, Cdc42, and CaV2.1 calcium channels. Neuron *61*, 556–569.

Gainey, M.A., Hurvitz-Wolff, J.R., Lambo, M.E., and Turrigiano, G.G. (2009). Synaptic scaling requires the GluR2 subunit of the AMPA receptor. J. Neurosci. *29*, 6479–6489.

Goold, C.P., and Davis, G.W. (2007). The BMP ligand Gbb gates the expression of synaptic homeostasis independent of synaptic growth control. Neuron *56*, 109–123.

Grubb, M.S., and Burrone, J. (2010). Activity-dependent relocation of the axon initial segment fine-tunes neuronal excitability. Nature *465*, 1070–1074.

Haghighi, A.P., McCabe, B.D., Fetter, R.D., Palmer, J.E., Hom, S., and Goodman, C.S. (2003). Retrograde control of synaptic transmission by postsynaptic CaMKII at the *Drosophila* neuromuscular junction. Neuron *39*, 255–267.

Harris, K.D., Hirase, H., Leinekugel, X., Henze, D.A., and Buzsaki, G. (2001). Temporal interaction between single spikes and complex spike bursts in hippocampal pyramidal cells. Neuron *32*, 141–149.

Hartman, K.N., Pal, S.K., Burrone, J., and Murthy, V.N. (2006). Activity-dependent regulation of inhibitory synaptic transmission in hippocampal neurons. Nat. Neurosci. *9*, 642–649.

Hessler, N.A., Shirke, A.M., and Malinow, R. (1993). The probability of transmitter release at a mammalian central synapse. Nature *366*, 569–572.

Ibata, K., Sun, Q., and Turrigiano, G.G. (2008). Rapid synaptic scaling induced by changes in postsynaptic firing. Neuron *57*, 819–826.

Isokawa, M., Levesque, M., Fried, I., and Engel, J., Jr. (1997). Glutamate currents in morphologically identified human dentate granule cells in temporal lobe epilepsy. J. Neurophysiol. *77*, 3355–3369.

Ishida, A., Kameshita, I., Okuno, S., Kitani, T., and Fujisawa, H. (1995). A novel highly specific and potent inhibitor of calmodulin-dependent protein kinase II. Biochem. Biophys. Res. Commun. *212*, 806–812.

Kandel, E.R., and Spencer, W.A. (1961). Electrophysiology of hippocampal neurons. II. After-potentials and repetitive firing. J. Neurophysiol. *24*, 243–259.

Kirov, S.A., and Harris, K.M. (1999). Dendrites are more spiny on mature hippocampal neurons when synapses are inactivated. Nat. Neurosci. *2*, 878–883.

Lisman, J., Schulman, H., and Cline, H. (2002). The molecular basis of CaMKII function in synaptic and behavioural memory. Nat. Rev. Neurosci. *3*, 175–190.

Magee, J.C., Avery, R.B., Christie, B.R., and Johnston, D. (1996). Dihydropyridine-sensitive, voltage-gated Ca2+ channels contribute to the resting intracellular Ca2+ concentration of hippocampal CA1 pyramidal neurons. J. Neurophysiol. *76*, 3460–3470.

Manabe, T., Wyllie, D.J., Perkel, D.J., and Nicoll, R.A. (1993). Modulation of synaptic transmission and long-term potentiation: Effects on paired pulse facilitation and EPSC variance in the CA1 region of the hippocampus. J. Neurophysiol. *70*, 1451–1459.

Marie, H., Morishita, W., Yu, X., Calakos, N., and Malenka, R.C. (2005). Generation of silent synapses by acute in vivo expression of CaMKIV and CREB. Neuron *45*, 741–752.

Meng, Y., Zhang, Y., and Jia, Z. (2003). Synaptic transmission and plasticity in the absence of AMPA glutamate receptor GluR2 and GluR3. Neuron *39*, 163–176.

Mu, Y., Otsuka, T., Horton, A.C., Scott, D.B., and Ehlers, M.D. (2003). Activity-dependent mRNA splicing controls ER export and synaptic delivery of NMDA receptors. Neuron *40*, 581–594.

Murphy, T.H., Worley, P.F., and Baraban, J.M. (1991). L-type voltage-sensitive calcium channels mediate synaptic activation of immediate early genes. Neuron *7*, 625–635.

Murthy, V.N., Schikorski, T., Stevens, C.F., and Zhu, Y. (2001). Inactivity produces increases in neurotransmitter release and synapse size. Neuron *32*, 673–682.

Nagel, G., Szellas, T., Huh, W., Kateriya, S., Adeishvili, N., Berthold, P., Ollig, D., Hegemann, P., and Bamberg, E. (2003). Channelrhodopsin-2, a directly light-gated cation-selective membrane channel. Proc. Natl. Acad. Sci. USA *100*, 13940–13945.

Nikolaev, A., McLaughlin, T., O'Leary, D.D., and Tessier-Lavigne, M. (2009). APP binds DR6 to trigger axon pruning and neuron death via distinct caspases. Nature *457*, 981–989.

O'Brien, R.J., Kamboj, S., Ehlers, M.D., Rosen, K.R., Fischbach, G.D., and Huganir, R.L. (1998). Activity-dependent modulation of synaptic AMPA receptor accumulation. Neuron *21*, 1067–1078.

Otis, T.S., Koninck, Y.D., and Mody, I. (1994). Lasting potentiation of inhibition is associated with an increased number of gamma-aminobutyric acid type A receptors activated during miniature inhibitory postsynaptic currents. Proc. Natl. Acad. Sci. USA *91*, 7698–7702.

Rao, A., and Craig, A.M. (1997). Activity regulates the synaptic localization of the NMDA receptor in hippocampal neurons. Neuron *19*, 801–812.

Sanhueza, M., McIntyre, C.C., and Lisman, J.E. (2007). Reversal of synaptic memory by Ca2+/Calmodulin-dependent protein kinase II inhibitor. J. Neurosci. *27*, 5190–5199.

Scheibel, M.E., Crandall, P.H., and Scheibel, A.B. (1974). The hippocampal-dentate complex in temporal lobe epilepsy. A Golgi study. Epilepsia *15*, 55–80.

Schiller, J., Major, G., Koester, H.J., and Schiller, Y. (2000). NMDA spikes in basal dendrites of cortical pyramidal neurons. Nature *404*, 285–289.

Seeburg, D.P., Feliu-Mojer, M., Gaiottino, J., Pak, D.T., and Sheng, M. (2008). Critical role of CDK5 and Polo-like kinase 2 in homeostatic synaptic plasticity during elevated activity. Neuron *58*, 571–583.

Shepherd, J.D., Rumbaugh, G., Wu, J., Chowdhury, S., Plath, N., Kuhl, D., Huganir, R.L., and Worley, P.F. (2006). Arc/Arg3.1 mediates homeostatic synaptic scaling of AMPA receptors. Neuron *52*, 475–484.

Song, I., and Huganir, R.L. (2002). Regulation of AMPA receptors during synaptic plasticity. Trends Neurosci. *25*, 578–588.

Soong, T.W., Stea, A., Hodson, C.D., Dubel, S.J., Vincent, S.R., and Snutch, T.P. (1993). Structure and functional expression of a member of the low voltage-activated calcium channel family. Science *260*, 1133–1136.

Stellwagen, D., and Malenka, R.C. (2006). Synaptic scaling mediated by glial TNF-alpha. Nature *440*, 1054–1059.

Swann, J.W., Al-Noori, S., Jiang, M., and Lee, C.L. (2000). Spine loss and other dendritic abnormalities in epilepsy. Hippocampus *10*, 617–625.

Takemoto-Kimura, S., Ageta-Ishihara, N., Nonaka, M., Adachi-Morishima, A., Mano, T., Okamura, M., Fuhjii, H., Fuse, T., Hoshino, M., Suzuki, S., et al. (2007). Regulation of dendritogenesis via a lipid-raft-associated Ca2+/Calmodulin-dependent protein kinase CLICK-III/CaMK1gamma. Neuron *54*, 755–770.

Thiagarajan, T.C., Lindskog, M., and Tsien, R.W. (2005). Adaptation to synaptic inactivity in hippocampal neurons. Neuron *47*, 725–737.

Thiagarajan, T.C., Piedras-Renteria, E.S., and Tsien, R.W. (2002). alpha- and betaCaMKII: Inverse regulation by neuronal activity and opposing effects on synaptic strength. Neuron *36*, 1103–1114.

Tokumitsu, H., Inuzuka, H., Ishikawa, Y., and Kobayashi, R. (2003). A single amino acid difference between alpha and beta Ca2+/calmodulin-dependent protein kinase kinase dictates sensitivity to the specific inhibitor, STO-609. J. Biol. Chem. *278*, 10908–10913.

Tsien, R.W., Lipscombe, D., Madison, D.V., Bley, K.R., and Fox, A.P. (1988). Multiple types of neuronal calcium channels and their selective modulation. Trends Neurosci. *11*, 431–438.

Turrigiano, G., Abbott, L.F., and Marder, E. (1994). Activity-dependent changes in the intrinsic properties of cultured neurons. Science *264*, 974–977.

Turrigiano, G.G. (2008). The self-tuning neuron: Synaptic scaling of excitatory synapses. Cell *135*, 422–435.

Turrigiano, G.G., Leslie, K.R., Desai, N.S., Rutherford, L.C., and Nelson, S.B. (1998). Activity-dependent scaling of quantal amplitude in neocortical neurons. Nature *391*, 892–896.

Turrigiano, G.G., and Nelson, S.B. (2000). Hebb and homeostasis in neuronal plasticity. Curr. Opin. Neurobiol. *10*, 358–364.

Watt, A.J., van Rossum, M.C., MacLeod, K.M., Nelson, S.B., and Turrigiano, G.G. (2000). Activity coregulates quantal AMPA and NMDA currents at neocortical synapses. Neuron *26*, 659–670.

Wayman, G.A., Impey, S., Marks, D., Saneyoshi, T., Grant, W.F., Derkach, V., and Soderling, T.R. (2006). Activity-dependent dendritic arborization mediated by CaM-kinase I activation and enhanced CREB-dependent transcription of Wnt-2. Neuron *50*, 897–909.

Wayman, G.A., Lee, Y.S., Tokumitsu, H., Silva, A., and Soderling, T.R. (2008). Calmodulin-kinases: Modulators of neuronal development and plasticity. Neuron *59*, 914–931.

Westenbroek, R.E., Ahlijanian, M.K., and Catterall, W.A. (1990). Clustering of L-type Ca2+ channels at the base of major dendrites in hippocampal pyramidal neurons. Nature *347*, 281–284.

Wierenga, C.J., and Wadman, W.J. (1999). Miniature inhibitory postsynaptic currents in CA1 pyramidal neurons after kindling epileptogenesis. J. Neurophysiol. *82*, 1352–1362.

Wu, G.Y., Deisseroth, K., and Tsien, R.W. (2001). Activity-dependent CREB phosphorylation: Convergence of a fast, sensitive calmodulin kinase pathway and a slow, less sensitive mitogen-activated protein kinase pathway. Proc. Natl. Acad. Sci. USA *98*, 2808–2813.

Zhang, Y.P., and Oertner, T.G. (2007). Optical induction of synaptic plasticity using a light-sensitive channel. Nat. Methods *4*, 139–141.